European Polymer Journal 45 (2009) 2653–2664

Contents lists available at ScienceDirect

European Polymer Journal

journal homepage: www.elsevier.com/locate/europolj

Structure and properties of new polyester elastomers composed of poly(trimethylene terephthalate) and poly(ethylene oxide)

Anna Szymczyk *

Institute of Physics and Institute of Materials Science and Engineering, West Pomeranian University of Technology, Al. Piastów 17, 70-310 Szczecin, Poland

ARTICLE INFO

Article history:
Received 25 January 2009
Received in revised form 10 April 2009
Accepted 29 May 2009
Available online 6 June 2009

Keywords:
Poly(trimethylene terephthalate)
Poly(ethylene oxide)
Polycondensation
Polyester thermoplastic elastomers

ABSTRACT

Series of PTT-*b*-PEO copolymers with different composition of rigid PTT and PEO flexible segments were synthesized from dimethyl terephthalate (DMT), 1,3-propanediol (PDO), poly(ethylene glycol) (PEG, M_n = 1000 g/mol) in a two stage process involving transesterification and polycondensation in the melt. The weight fraction of flexible segments was varied between 20 and 70 wt%. The molecular structure of synthesized copolymers was confirmed by ^{1}H NMR and ^{13}C NMR spectroscopy. The superstructure of these polymers was characterized by DSC, DMTA, WAXS and SAXS measurements. It was observed that domains of three types can exist in PTT-*b*-PEOT copolymers: semi-crystalline PTT, amorphous PEO rich phase (amorphous PEO/PTT blended phase) and semi-crystalline PEO phase. Semi-crystalline PEO phase was observed only at temperature below 0 °C for sample containing the highest concentration of PEO segment. The phase structure, thermal and mechanical properties are effected by copolymer composition. The copolymers containing 30÷70 wt% of PEO segment posses good thermoplastic elastomers properties with high thermal stability. Hardness and tensile strength rise with increase of PTT content in copolymers.

1. Introduction

Poly(trimethylene terephthalate) (PTT) is an semi-crystalline polyester of renewed interest on account of a recent breakthrough in low-cost production of the monomer 1,3-propanediol (PDO), which enabled PTT to be produced at costs appropriate for commercialization. Commercially available PTT is produced by Shell Chemicals (Corterra®) and DuPont (Sorona, Biomax® PTT) [1–5]. The production of PTT by Shell Chemicals is based on the PDO obtained by process of hydroformylation of ethylene oxide. Sorona PTT produced by DuPont and Tate & Lyle is based on a new developed process that uses renewable sources (corn sugar) to manufacture "bio"-PDO. The bio route of PDO production consumes 40% less energy and reduces greenhouse gas emissions by 20% versus petroleum-based PDO [5].

PTT possesses several advantageous properties, including good tensile behavior, resilience, outstanding elastic recovery, and ability to be colored with different dies. These characteristics make PTT highly suitable for uses in engineering thermoplastic applications as fibers or films. Therefore, PTT has recently attracted several investigators for its characteristics either in pure state [6–9], in copolymer systems [10–12], in blends [13–15] and nanocomposites [16–19].

Multiblock copolymers which show thermoplastic and elastic behavior are composed of two types of blocks: flexible blocks phase (soft phase) with a low glass transition temperature and rigid, glassy or crystalline blocks, which provide physical crosslinking. Due to the two-phase microstructure, thermoplastic elastomers possess excellent mechanical properties, such as low-temperature flexibility, impact strength, toughness and high modules in the rubbery plateau region. At higher temperatures, the dissociation of the physical bonds occur and copolymers become soft and flow like a thermoplastic material, enabling them

* Tel.: +48 91 449 44 05; fax: +48 91 43 42 113.
E-mail address: anna.szymczyk@zut.edu.pl

0014-3057/$ - see front matter © 2009 Elsevier Ltd. All rights reserved.
doi:10.1016/j.eurpolymj.2009.05.032

to be processed in the melt phase by using conventional techniques such as injection molding. An industrially important class of thermoplastic elastomers (TPEs) are the segmented block copoly(ether-esters). Commercially available polyester TPEs are composed of poly(butylene terephthalate) PBT as polyester segment and poly(tetramethylene oxide) (PTMO) (Hytrel, DuPont; Arnitel, DSM) as polyether flexible segments [20].

In this work, the PTT was used as the rigid segment in multiblock copoly(ether-ester)s, while poly(ethylene glycol) (PEG) was used as the flexible segment. PEG is nontoxic, non-antigenic, non-immunogenic, semi-crystalline polymer with glass transition temperature below zero [21–23], which is often applied as the component to impart good hydrophilicity as well as biocompatibility of biomaterials.

This is the first report on this system and it is of general interest, as thermoplastic copoly(ether-ester)s, especially with improved elasticity, are currently in the focus of industrial research. These new system can have potential applications as biomaterials for example, to fabricate scaffold for bone cartilage, and skin tissue engineering, or as anti-adhesion barrier etc. [23–26]. Therefore, the combined properties of these two semi-crystalline polymers, i.e., rigid hydrophobic semi-crystalline PTT segments and hydrophilic semi-crystalline flexible PEO segments can be interesting for future applications. Here, denotation PEO for poly(ethylene oxide) in polymer chain and PEG for polyether terminated by hydroxyl groups i.e., poly(ethylene glycol) is used. The influence of PEO flexible segment content on the resulting PTT-*b*-PEO copolymers properties, such phase structure, thermal and mechanical properties is investigated.

2. Experimental

2.1. Materials

Dimethyl terephthalate (DMT) (Aldrich) and Irganox 1010 (Ciba-Geigy, Switzerland) were used as received, without further purification. 1,3-propanediol (Shell Chemicals Europe B.V., The Netherlands) was distilled before using. Poly(ethylene glycol) (PEG) with molecular weight of 1000 g/mol was purchased from Polysciences Inc., and as catalyst titanium (IV) butoxide (TBT; $\geqslant$97.0%) from Fluka was used.

2.2. Synthesis of PTT-b-PEO copolymers

PTT-*b*-PEO copolymers were prepared with several different PTT/PEO weight ratios from DMT, PDO and PEG in two steps: the first involved the transesterification of DMT by PDO forming bis-(3-hydroxypropylene) terephthalate (BHPT), the second was melt polycondensation of BHPT with PEG. Both of steps were carried out in presence of TBT (0.25 wt% in relation to DMT) as catalyst in a 1 L high pressure reactor (Autoclave Engineers Pennsylvania, USA) equipped with a vacuum pump, condenser, and cold trap for collecting the by-products. In the first step the reactor was charged with DMT and PDO with the desired ratios, and catalyst. The molar ratio of the diester (DMT) and diol (PDO) was 1:1.5. The transesterification reaction, was carried out under a constant flow of nitrogen at temperature of 160–165 °C for one and half hour. During the reaction, methanol was distilled and collected as a by-product. The conversion of the transesterification reaction was calculated by monitoring the amount of effluent methanol. When the distillation of methanol ceases, the reaction was completed and produced BHPT and monohydroxypropl terephthalate (MHPT) was gradually heated to 210 °C. Then, the PEG and thermal stabilizer (Irganox 1010, 0.5 wt% in relation to total comonomer mass) were introduced to the reactor. The reaction temperature was increased to 250–255 °C for the polycondensation reaction. Vacuum was applied gradually and the final pressure was lower than 25 Pa. The stirring torque change was monitored in order to estimate the melt viscosity of the product at temperature of 255 °C. The reaction was stopped when the torque no longer increased. The polycondensation reaction time was 2–3 h dependent form the weight content of PEO segments. The product was extruded into cold water through a drain valve. The PTT homopolymer was synthesized following the same procedure. The produced copolymer samples were coded as PEE-*x*, where *x* describe the weight content of PEO blocks, respectively.

2.3. Sample preparation

Before molecular, intrinsic viscosity and thermal characterization samples were purified by means using the following procedure: after dissolution in 1,1,1,3,3,3-hexafluoro-2-propanol and precipitation in methanol, they were recovered by filtration and again dissolved and reprecipitated twice, and then dried under vacuum at temperature of 50 °C for 48 h. Samples for WAXS, SAXS, DMTA, hardness and tensile tests were prepared by injection moulding machine (Boy 15, Germany) at temperature of approximately 20 °C higher than melting temperature determined by DSC and at pressure of injection of 50 MPa and a holding down pressure of 20 MPa for 20 s; the temperature of the mould was set at 30 °C.

2.4. Characterization of polymers

The inherent viscosity [η] of the polymers was determined at 30 °C using a capillary Ubbelohde type I_c (K = 0.03294). The polymer solution had a concentration of 0.5 g/dl in mixture (60/40 by weight) phenol/1,1,2,2-tetrachloroethane. The Mark–Houwink relationship $[\eta] = 5.36 \times 10^{-4} \times M_w^{0.69}$ [27] was used to calculate molecular weight and degree of polymerization (where $x = M_n/206$, $M_w/M_n = 2$) of PTT homopolymer.

Hardness measurements were performed according to a standard DIN 53505 and ISO 868 on a Shore D apparatus (Karl Frank GmbH, Type 104, Germany).

The melt flow rate (MFR) was measured by using a melt indexer (CEAST, Italy) as weight of melt flow in grams per 10 min, at temperature above the melting point (listed in Table 1) at orifice diameter 2.095 mm and under 21.18 N load, according to ISO 1133 specification.

Table 1
Characteristic of PTT-*b*-PEO copolymers.

Sample	w_{PEO}, wt%	*x*, mol/mol	Yield, %	[η], dl/g	MFR(*T*), g/10 min	*H*, Sh D
PTT	0	101.9[B]	94	0.83	20.1 (230 °C)	80
PEE-20	20	21.94	97	1.03; 1.01[E]	3.4 (220 °C)	72
PEE-30	30	12.80	93	1.16; 1.18[E]	2.8 (215 °C)	65
PEE-40	40	8.23	96	1.29; 1.27[E]	10.8 (210 °C)	57
PEE-50	50	5.48	98	1.34; 1.36[E]	19.4 (200 °C)	52
PEE-60	60	3.65	94	1.43; 1.43[E]	21.5 (190 °C)	44
PEE-70	70	2.35	92	1.47; 1.45[E]	21.3 (180 °C)	32

w_{PEO}, weight fraction of PEO segments; *x*, degree of polymerization of rigid segment with reference of 1 T-PEO unit; B, for PTT estimated from the measured intrinsic viscosity [27], for PEE calculated form the composition; [η], intrinsic viscosity, E, after extraction; MFR(*T*), melt flow rate at temperature *T* (°C); *H*, hardness.

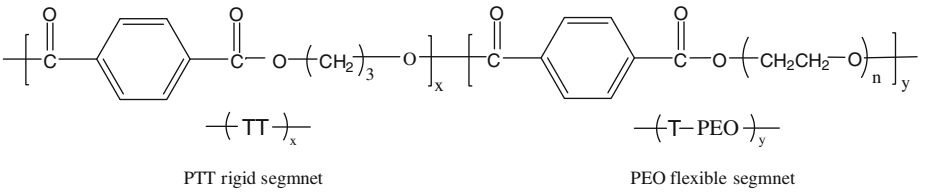

Fig. 1. Structure PTT-*b*-PEO copolymers.

2.5. ^1H and ^{13}C nuclear magnetic resonance spectroscopy (NMR)

For ^1H NMR and ^{13}C NMR measurements a Bruker 400 MHz spectrometer was used. CF_3COOD was used as solvent and tetramethylsilane (TMS) as internal reference. The areas (or intensity in the ^{13}C NMR) of characteristic peaks were used to determine weight and mole fraction constituent of copolymers before and after extraction. The weight fraction of flexible segment (PEO) was calculated from the integral intensities *d* and *b* (see Fig. 2) corresponding to CH_2–O–CH_2 and $CH_2CH_2CH_2OCO$ proton resonances, respectively as following equation:

$$w_{PEO}, \mathrm{wt}\% = \frac{44(d/4)}{44(d/4) + 206(b/4)} \times 100\% \quad (1)$$

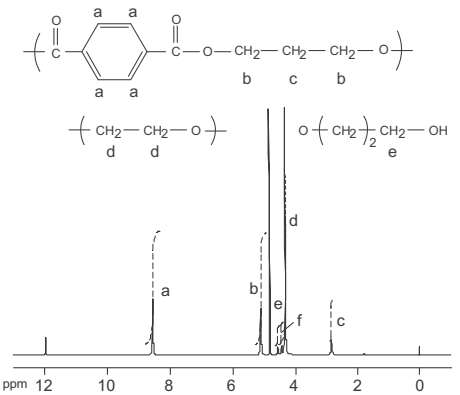

Fig. 2. ^1H NMR spectra of PEE-50 copolymer (before extraction) in CF_3COOD.

where 44 and 206 are the molecular weight of the flexible polyether and rigid polyester chain repeat unites, respectively. The Eq. (1) was used also to calculate the weight fraction of PEO segments based on ^{13}C NMR spectra, where $d/4 = I_1/2$ and $b/4 = I_2/2$ and the intensities I_1 and I_2 (see Fig. 3) correspond to the carbon signals of CH_2–O–CH_2 and COO groups, respectively. The mole fraction of the soft segments was calculated using the following equation:

$$w_{PEO}, \mathrm{mol}\% = \frac{44(d/85.27)}{44(d/85.27) + 206(b/4)} \times 100\% \quad (2)$$

where 85.27 and 4 are numbers of protons in the corresponding repeating units. From ^{13}C NMR spectra, the mole fraction of the flexible segments was determined by using the equation:

$$w_{PEO}, \mathrm{mol}\% = \frac{(I_1/44.46)}{(I_1/44.46) + (I_2/2)} \times 100\% \quad (3)$$

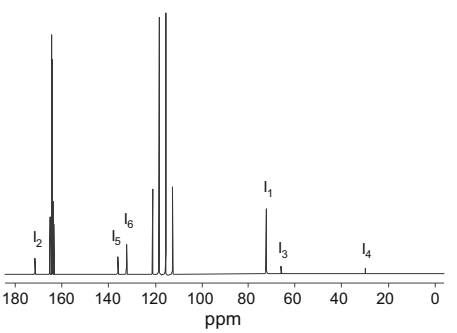

Fig. 3. ^{13}C NMR spectra of PEE-50 copolymer (before extraction) in CF_3COOD.

where 44.46 and 2 are the numbers of carbons in the corresponding repeating units. The weight (and mole) fraction of rigid segments was calculated by subtraction of the weight (mole) content of the flexible segments from 100%.

2.6. Tensile tests

The tensile properties were of the samples were measured with an Instron 1112 tensile testing machine operated at a constant crosshead speed of 50 mm/min. Measurements were performed at room temperature on dumbbell samples. According to DIN 53455 standards, the values of Young's modulus (E), stress and strain at break were determined from stress–strain curves on an average of five specimens for each kind of materials.

2.7. Thermal analysis by DSC and TMDSC

Differential scanning calorimetry (DSC) measurements were carried out with a TA Q-100 Instrument Universal Analysis 2000 system. The measurements were taken over a temperature range of $-90 \div 250$ °C using the so-called triple cycle, "heating–cooling–heating", at a rate of 10 °C/min, under nitrogen flow. Additionally for PEE-50 sample, the temperature-modulated (TMDSC) curves were recorded during heating with a modulated signal at a heating rate of 3 °C/min and with a modulation of ±0.48 °C every 60 s. The crystallization and melting temperatures (T_c, T_m) were measured at the maximum of the endo- and exo-thermic peaks, respectively, and the glass transition temperatures (T_g) were taken as the midpoint of the change in heat capacity ($\Delta c_p/2$). The degree of crystallinity (x_c) of the copolymers to content of PTT was calculated in terms of the following expression:

$$x_c = (\Delta H_m/\Delta H_m^0 \cdot w_r) \cdot 100\%$$

in which ΔH_m denotes the melt crystallization enthalpy of the component in the sample, w_r refers to the weight fraction of the rigid segment content, and ΔH_m^0 is the enthalpy of fusion of 100% crystalline component based on the literature data (for PTT, ΔH_m = 146 J/g [6]).

2.8. Thermogravimetric analysis (TGA)

The TGA analyses were carried out on a SETARAM TGA 92-16 apparatus. The TGA (weight loss in % versus temperature) curves and the first derivative of the TGA (DTG) curves where conducted at $25 \div 700$ °C, at heating rate of 10 °C/min under an argon and under dray air (N_2:O_2 = 80/20 vol/vol) atmosphere with flux rate of 20 mL/min.

2.9. Dynamical mechanical thermal analysis (DMTA)

The storage modulus (E'), loss modulus (E'') and the loss tangent (tan δ) were measured as a function of temperature with a Polymer Laboratories MK II dynamic mechanical thermal analyzer working in a bending mode at a frequency of 1 Hz. The samples were first cooled to −100 °C and, then subsequently heated at a rate of 3 °C/min. The glass transition temperature was taken as the temperature at the maximum relaxation peak of the loss modulus and tan δ curves. The softening/flow temperature (T_{flow}) was defined as the temperature at which the storage modulus reached 10 MPa.

2.10. X-ray analysis

Wide-angle X-ray scattering (WAXS) measurements of the samples were carried using a Seifert XDR 3000TT diffractometer equipped with computerized data collection and analytical tools. The X-ray source (CuK_α radiation, wavelength λ = 1.54 Å) was generated using an applied voltage of 40 kV and a filament current of 35 mA. CuK_α radiation was monocromized with a graphite monocromatizer and a Ni filter. The curves were recorded in the 2θ range 4–60° with a step of 0.01°. The degree of crystallinity was calculated using a modified Hindeleh & Johnson method [28] and a computer program WAXSFIT [29]. By means of the program, a linear background was subtracted and diffraction curves were resolved into crystalline and amorphous components. The resolution was performed using a multiobjective optimization procedure and a hybrid system that combined genetic algorithms and classical optimization method.

A Bruker NanoStar SAXS (small angle X-ray scattering) system with a pinhole collimation and two-dimensional detector (HiSTAR) was employed for data collection. The X-ray radiation employed was generated from a Cu rotating anode fine-focus X-ray source (K_α = 1.5418 Å with a potential of 40 kV and a current of 35 mA). The SAXS curves were recorded in the range 0.1 $nm^{-1} < q < 2.6$ nm^{-1}. The position of the scattering maximum (q_{max}), from the Lorentz-corrected SAXS profile, was used for the calculation of the Bragg's long period (L),

$$L = 2\pi/q_{max},$$

where $q = (4\pi/\lambda)\sin\theta$ is the scattering vector, and 2θ is the scattering angle. L represents the average periodicity of the lamellar stack, which corresponds, in that approximation to the sum of the crystal lamellae and of the interlamellar amorphous regions.

3. Results and discussion

A series of thermoplastic poly(ether-ester)s based on rigid PTT and flexible PEO segments, PTT-*b*-PEO, was synthesized by a catalyzed two-step reaction, involving transesterification and polycondensation in the bulk. The syntheses were carried out with a highly effective catalyst, $Ti(OBu)_4$, with the addition of Irganox 1010 as an antioxidant. The structural formula of the synthesized random block PTT-*b*-PEO copolymers is shown in Fig. 1. The PTT–PEO copolymer can be present as random copolyester (TT units and T-PEO units). It gives possibility to calculate the degree of polymerization (polycondensation) rigid segment $(TT)_x$. The theoretical chemical composition of a series of PTT-*b*-PEO copolymers, yields after precipitation in methanol, and its basic physical properties as intrinsic viscosity [η], melt flow rate (MFR) and hardness are summarized in Table 1. The average length x (degree of

polymerization) of the rigid PTT segment was calculated according to 1 mol ($y = 1$ in Fig. 1) of flexible T–PEO (T for terephthalate unit) segments. The degree of polymerization of the rigid segments (Table 1), calculated from the reaction mixture compositions, is ranged from 21.9 (PEE-20) to 2.4 (PEE-70). All syntheses of homopolymer PTT and PTT-*b*-PEO copolymers were finished, when the reaction mixture rich the same value of melt viscosity, which was estimated by monitoring of change of the stirring torque. For almost all the copolymers, the yield after precipitation in methanol was above 90%. The values of limiting viscosity number (Table 1) for copolymers after and before precipitation in methanol were the same or very close, that can suggest that almost all the monomers are incorporated into the polymer chains, both in the rigid and flexible segments. The limiting viscosity number of polymers is influenced by the molecular chain weight and flexibility of the macromolecular chain. The $[\eta]$ of the synthesized copolymers after extraction are between 1.02 dl/g and 1.45 dl/g for copolymers and 0.83 dl/g for the homopolymer PTT. The synthesized homopolymer PTT have a number average molecular weight of 42,000 g/mol, calculated from the measured intrinsic viscosity using the Mark–Houwink equation with constants a and k determined previously [27]. The Mark–Houwink constants are not known for new PTT-*b*-PEO copolymers, therefore values of $[\eta]$ are used for comparison. Hardness and temperature at which the polymers melt and flow (MFR) are depended on the copolymer composition.

3.1. NMR analysis of structure and composition

The molecular structure of the synthesized PTT-*b*-PEO copolymers was confirmed by ^{1}H NMR and ^{13}C NMR spectroscopy. A typical ^{1}H NMR and C–^{13}C NMR spectra of PTT–PEO copolymer (PEE-50 before extraction) are shown in Figs. 2 and 3. In ^{1}H NMR spectra, the signals at 8.59 ppm (peak *a*; 4H, doublet) correspond to the aromatic proton of the terephthalate units. The chemical shifts at 5.09 ppm (peak *b*; 4H, $C\underline{H}_2$–CH_2–$C\underline{H}_2$) and at 2.82 ppm (peak *c*; 2H, CH_2–$C\underline{H}_2$–CH_2) were for the methylene protons of the short chain diol (PDO). The signals of the proton on the carbon atoms connected with oxygen $C\underline{H}_2$–O–$C\underline{H}_2$ of the PEO repeating blocks, appear at 4.32 ppm (peak *d*). Small signals at 5.53 ppm (peak *e*) and at 4.43 ppm (peak *f*) are due to the protons of methylene in CH_2–OH end groups of polyester and polyether, respectively. Besides, the two signals at: 11.08 and 4.79 ppm were from solvent and from water, respectively. In ^{13}C NMR (Fig. 3) spectra, the signals from the flexible segment $\underline{C}H_2$–O carbons appear at 72.18 ppm (peak I_1), and the signals from carbons in short chain glycol appears at 29.74 ppm (peak I_4) and 65.98 ppm (peak I_3). The signals at: 171.34 (I_2), 136.02 (I_5) and 132.41 (I_6) ppm correspond to the carbonyl group (COO) and aromatic carbons of polyester units, respectively. The presented representative spectra for PEE-50 (before extraction) are consistent with the expected structure, indicating that no side reactions occur during synthesis of the samples under investigations.

The weight and mole fraction of flexible and rigid segments were calculated from the ^{1}H NMR and ^{13}C NMR spectra according to Eqs. (1)–(3) and are given in Table 2. The average length of the rigid PTT segments were also calculated from the ratio (d:a or I_1:I_2) of the peak intensities, based on the assumption that the flexible segment length is equal to the length of the staring PEO. The calculated degree of polymerization of the PTT (x) segments in the macro-chain from ^{1}H NMR spectra was between 22.25 (PEE-20) and 2.66 (PEE-70). Values of the average degree of polymerization of the rigid segments calculated from ^{13}C NMR spectra were lower than determined form ^{1}H NMR spectra. The obtained results show that in all copolymers the content of the flexible segments was lower than would be expected from the composition of the reaction mixture. For all the samples with exception of PEE-60 and PEE-70, the difference between the experimental and theoretical composition was less than 5%. This values were in the range of the experimental error of the determination of the composition by NMR spectroscopy. The determined lower content of the flexible PEO segments than calculated theoretically from the mixture of starting materials for PEE-60 and PEE-70 copolymers, can be explained that not all PEG units (extracted during purification) were built into macro-chain.

The molecular weight of the repeating units $\overline{M}_{ru}$ of the synthesized PTT-*b*-PEO copolymers, was calculated from following equation:

$$\overline{M}_{ru} = x \cdot 206 + y \cdot 1130, \mathrm{g/mol}$$

where x and y were the mole content of rigid PTT and flexible T-PEO segments, respectively. The predicted from ^{1}H NMR spectra values of the molecular weight of the

Table 2
The composition of the synthesized PTT–PEO copolymers determined from ^{1}H NMR and ^{13}C NMR spectra.

Sample	Flexible segment		x	Rigid segment	
	mol%	wt%	mol/1 mol T-PEO	mol%	wag%
PEE-20	4.30	18.05	22.25	95.70	81.95
PEE-30	6.83; 7.41^C	25.95; 26.26^C	13.64; 12.49^C	93.17; 92.50^C	74.05; 73.74^C
PEE-40	10.32	36.54	8.68	89.68	63.46
PEE-50^{BE}	14.15; 18.55^C	43.09; 46.93^C	6.06; 4.39^C	85.85; 81.45^C	56.91; 53.07^C
PEE-50	14.33; 18.40^C	46.70; 46.73^C	5.97; 5.32^C	85.67; 81.60^C	53.30; 53.27^C
PEE-60	19.79	53.75	4.05	80.21	46.25
PEE-70	27.26; 30.60^C	63.38; 67.77^C	2.66; 1.28^C	72.74; 69.40^C	36.62; 32.23^C

w_{PEO}, weight fraction of PEO segments; x, degree of polymerization of rigid segment with reference of 1 mol of T-PEO unit; BE, before extraction; C, determined from C–^{13}C NMR spectra.

Table 3
The average molecular weight of the synthesized PTT–PEO copolymers determined from ^{1}H NMR spectra.

Sample	$\bar{M}_{ru}$, g/mol	$\bar{M}^T_{ru}$, g/mol	b	$\bar{M}_n$, g/mol
PTT	–	–	–	21,000[A]
PEE-20	5714	5650	4.17	23,977
PEE-30	3939, 3499[C]	3767	4.39	17,442
PEE-40	2918	2825	4.21	12 435
PEE-50[BE]	2378; 2034[C]	2336	4.97	11,969
PEE-50	2360; 2043[C]	2336	4.90	11,714
PEE-60	1964	1882	5.05	10,068
PEE-70	1678; 1392[C]	1614	5.88	10,017

A, determined from [η]; BE, before extraction; C, determined from C–^{13}C NMR spectra, $\bar{M}_{ru}$, $\bar{M}^T_{ru}$ – molecular weight of repeating units determined from ^{1}H and ^{13}C NMR spectra and calculated theoretically, respectively; b, number of repeating units; $\bar{M}_n$, average molecular weight of polymer determined from end group.

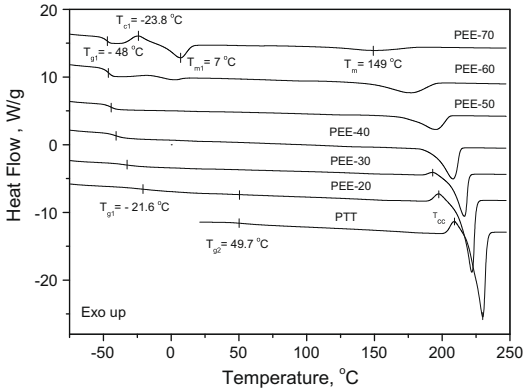

Fig. 5. DSC thermograms of PTT-*b*-PEO copolymers with different wt% contents of PTT segments in the polymer at heating rate 10 °C/min.

repeating units (Table 3) are very near to the calculated theoretically. The average number of repeating units b was calculated using the following equation:

$$b = 10^3(4I_a/4 \cdot I_e \cdot x \cdot M_{DMT})$$

where I_a and I_e were the intensities of proton resonance of terephthalate residue and end groups ($C\underline{H}_2OH$), respectively, and M_{DMT} = 194 g/mol. The average molecular weight of the polymer, $\bar{M}_n$ (Table 3), was calculated using the equation:

$$\bar{M}_n = b \cdot \bar{M}_{ru} + 2M_E, g/mol$$

where b and $\bar{M}_{ru}$ were calculated and are given in Table 3; M_E (O–$(CH_2)_3$–OH) = 75 g/mol. The synthesized copoly(ether-ester)s, have number average molecular weights estimated from 10,000 to 23,000 g/mol.

3.2. Phase structure and morphology

In PTT-*b*-PEO copolymers, the PTT and PEO segments may segregate into separate phases in the solid state as other segmented copolymers do due to the thermodynamic immiscibility of the rigid and flexible segments. The existence of a hetero-phase structure in these copolymers, which is the result of semi-crystalline and amorphous domains, was shown and confirmed by thermal analysis. The DSC thermograms of the samples are shown in Figs. 4–6 and the results are summarized in Table 4. Temperature-modulated DSC for PEE-50 sample (Fig. 4) showed that in these copolymers are present three phases; two amorphous phases (T_{g1}, T_{g2}) and one crystalline phase (T_m). The actual phase structure depended on the chemical composition. The first glass transition (T_{g1}) in low-temperature region corresponded to the amorphous PEO-rich phase (or amorphous PEO/PTT blended phase) and the second glass transition (T_{g2}) was attributed to amorphous rigid polyester sequences in the semi-crystalline hard phase. The melting point derived from the crystallized rigid segments (T_m) can be observed in the DSC curves of most samples. Besides, as can be seen in Fig. 4, in the non-reversible heat flow curve (C) in temperature range above 65 °C, there was an exotherm (cold crystallization) followed by an endotherm, since the non reversible component is kinetic in nature and can be attributed to non-reversible melting and crystallization on heating. The existence of two processes of recrystallization and melting on heating was confirmed. This endothermic peak in non-reversible heat flow curve (C) is corresponding to the endothermic peak in the in the reversible peak (curve

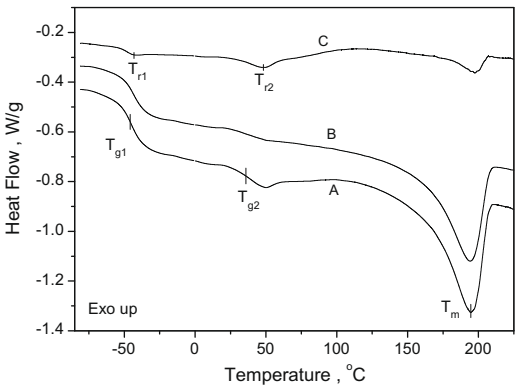

Fig. 4. Temperature modulated DSC curves for PEE/50 copolymer; (A) total, (B) reversible and (C) non-reversible heat flow.

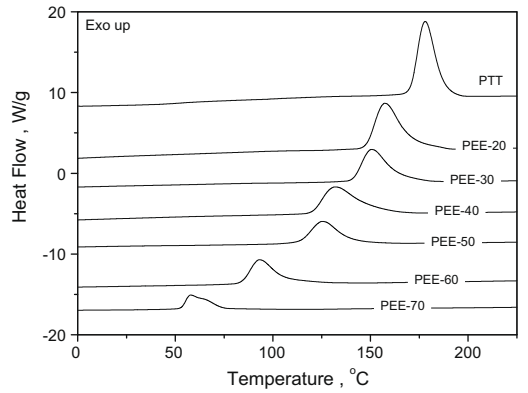

Fig. 6. DSC thermograms of PTT-*b*-PEO copolymers with different wt% contents of PTT segments in the polymer at cooling rate 10 °C/min.

Table 4
Thermal properties of PTT-*b*-PEO copolymers.

Sample	T_{g1}, °C	Δc_{p1}, J/g °C	T_{g2}, °C	T_m, °C	ΔH_m, J/g	T_c, °C	ΔHc, J/g	x_c, %	x_c^h, %
PTT	–	–	49.7	229.4	53.3	177.8	53.4	36.5	36.5
PEE-20	−21.6	0.20	49.3	221.9	42.6	157.2	42.9	29.2	36.5
PEE-30	−33.5	0.25	50.6	216.4	38.2	150.5	38.4	26.2	37.4
PEE-40	−40.8	0.32	51.1	208.0	33.4	131.6	33.6	22.8	38.0
PEE-50	−44.8	0.41	49.0	195.4	27.4	125.2	27.4	18.8	37.6
PEE-60	−46.7	0.51	44.3	176.5	20.5	93.0	20.4	14.0	35.0
PEE-70	−48.1	0.52	47.2	148.7	13.5	57.8	14.0	9.2	30.7

T_{g1}, glass transition temperature of soft phase; Δc_{p1}, change of heat capacity of flexible segments; T_{g2}, glass transition of amorphous part in semi-crystalline hard phase; T_m, ΔH_m, melting and crystallization temperature; T_c, ΔH_c, temperature and enthalpy of crystallization of hard phase; x_c, degree of crystallinity of the sample; $x_c^h = x_c/w_h$, degree of crystallinity with reference to rigid segments content.

B), i.e., they represent the non-reversible and reversible component melting of recrystallized polyester segments, respectively. The presence of non-reversing endothermic signal is typically due to complete melting of separate lamellae or stacks of lamellae and was also found in thermal analysis of several semi-crystalline polymers [30,31]. This is observed if melting temperature of prefect crystals is not too far from their equilibrium melting point. The crystals cannot recrystallize fast enough because of a low degree of under cooling. This slow recrystallization kinetics lead to high levels of non-reversing melting in heating scan. Additionally, on non-reversing curve two small endothermic peaks were seen at temperatures T_{r1} ($\sim T_{g1}$) and T_{r2} ($\sim T_{g2}$) representing the imaginary (energy loss or c_p'') part of complex specific heat c_p^*. According the to Schawe theory [32] the complex specific heat (c_p^*) signal on temperature MDSC is a sum of real c_p' (energy storage) and imaginary c_p'' (energy loss) parts, i.e., $c_p^* = c_p' + ic_p''$.

For sample containing 70 wt% of PEO, above the T_{g1} the crystallization ($T_{c1} = -17.7$ °C, $\Delta H_{c1} = 8.6$ J/g) and melting ($T_{m1} = 7$ °C, $\Delta H_{m1} = 14.6$ J/g) of polyether semi-crystalline phase were observed. The glass transition temperature, T_{g1}, of soft phase was shifted to higher (Figs. 5–7) temperatures indicating the blending of the amorphous phase of non-crystallized PTT rigid segments with the flexible/soft PEO segments. The decrease of the Δc_{p1} at T_{g1} with the increasing of the PTT content confirmed that the composition of soft phase was change. For PTT homopolymer and copolymers with higher content rigid segments before melting of PTT crystallites the presence of cold crystallization ($T_{cc} = 208$ °C for PEE-20 and 198 °C for PEE-30) was observed. The melting temperatures shifted to lower values and the enthalpy of melting decreased with increasing content of flexible segments from 222 °C (PEE-20) to 148 °C (PEE-70), which is the expected behaviour of the copolymers. The temperatures of crystallization (Fig. 6) increased with the increase of the length of rigid segments. The total degree of crystallinity of the synthesized PTT-*b*-PEO copolymers are in the range from 29% to 9% (Table 4). The degree of crystallinity with reference to rigid segment contents x_c^h values varied between 38% and 30%. It appeared that crystallinity of hard phase copolymer attended to contents of PTT segments is almost independently from the composition and from the average PTT block length, with the exception of sample PEE-70 which shows a lower crystallinity of 30%. This sample contains PTT segments with a rather short average block length of three units.

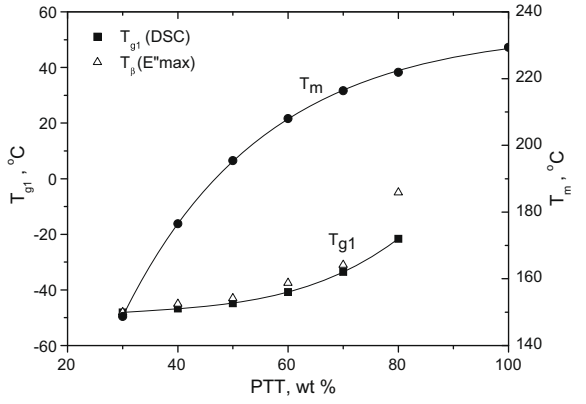

Fig. 7. Dependence of: melting temperature, glass transition temperature, β-relaxation temperature on weight fraction of the PTT rigid segments.

The dynamic mechanical properties of PTT and PTT-*b*-PEO copolymers as a function of temperature are shown in Fig. 8. The dynamic mechanical data are also summarized in Table 5. The loss modulus (E'') peak relaxation at −48 to −5 °C, corresponding to the glass relaxation (glass transition T_{g1} on DSC) temperature ($T_{\beta,}$) of the amorphous soft polyether phase moved to lower temperatures as the weight content of flexible segments in PTT-*b*-PEO copolymers increased. The PTT homopolymer have the α-relaxation at 59 °C corresponding to the glass transition of amorphous part in semi-crystalline hard phase. The little peak at about −80 °C on loss modulus and tan δ curves can be attributed to the relaxation processes involving the local motions of the carboxyl groups and the reorientation of the carboxyl groups in the amorphous phase [6]. The broad β-relaxation peaks suggests that this region can consist of a variety of processes probably related to the flexible and rigid segment length distribution. The decrease of T_β of soft phase with increasing of the flexible segments content was due to the increase of soft–hard phase separation. Additionally, for copolymers containing from 30–70 wt% of flexible segments, the typical plateau region in the storage modulus (E') plot between T_β of the soft phase and the softening temperature as usually found for elastic materials was also observed. For PEE-70, at temperature above the T_β, the storage modulus displayed a

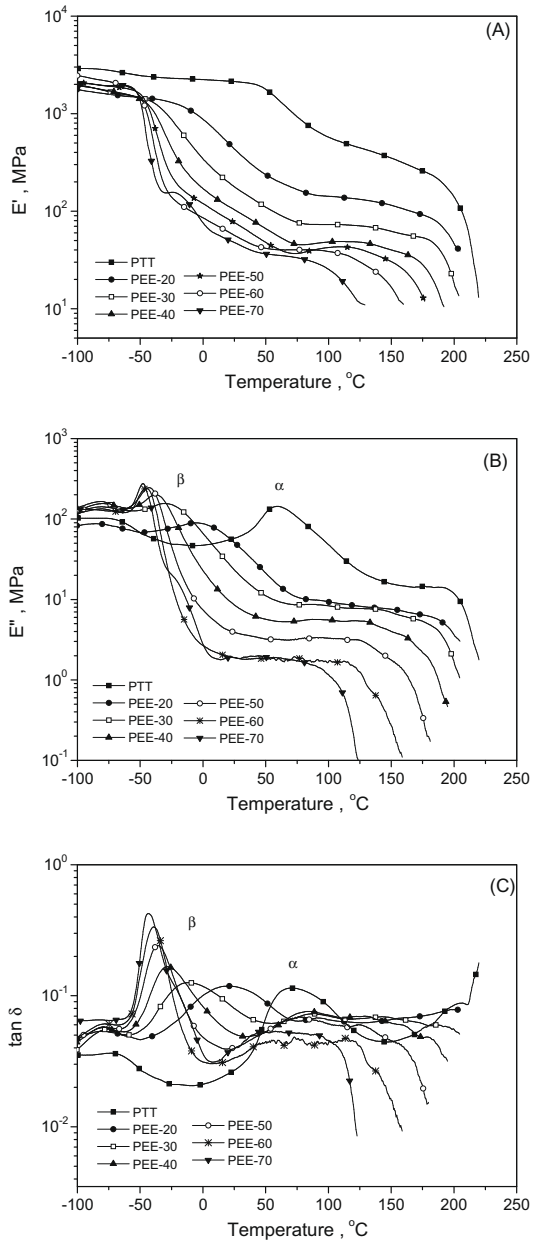

Fig. 8. The storage modulus E', loss modulus E'' and tan δ as a function of temperature for PTT-*b*-PEO copolymers.

shoulder before the start of the rubbery plateau and this was due to the presence of a crystalline PEO phase. Values of E' for PTT-*b*-PEO copolymers in the rubbery plateau was lower than the corresponding value for the homopolymer due to the presence of flexible segments and different degree of crystallinity.

In PTT-*b*-PEO copolymers depending on the rigid PTT segments content, a more or less continuous crystalline superstructure can be formed by single crystal lamellae tied together by short sequences of rigid segments. The crystal structure and the apparent degree of crystallinity for PTT and PTT-*b*-PEO block copolymers prepared by injection moulding were observed using WAXS and the results are shown in Fig. 9 and in Table 6. The peaks and corresponding reflections of PTT were observed at the scattering angles 2θ of ca. 15.3°, 16.8°, 19.4°, 21.7°, 23.6°, 24.6° and 27.3°, which correspond to the reflection planes of $(0\,1\,0)$, $(0\,\bar{1}\,2)$, $(0\,1\,2)$, $(1\,0\,\bar{2})$, $(1\,0\,2)$, $(1\,\bar{1}\,3)$, and $(1\,0\,\bar{4})$, respectively [33]. The calculated degree of crystallinity value (Table 6) for the copolymers was found to decrease from that of PTT with increasing flexible segments content. The reduction of the crystallinity degree is a result of change in the length of the rigid segments.

A well-defined SAXS peak were detected for the whole composition range (see Fig. 10) of PTT-*b*-PEO copolymers. The corresponding long period (L), derived from SAXS curves is reported in Table 6. The long period is a measure of the average distance between crystals and, as such, is the sum of the average thickness of the crystalline layers and amorphous regions. As well evidenced in Table 6, the L values increased by decreasing the degree of crystallinity of the sample, which was the consequence of increasing the flexible segments content. This results confirmed that the synthesized copolymers were characterized by a less favourable perfection of crystals with involvement of PEO. The amorphous phase domains consisted of sub-domains of polyester and flexible segments. The rise of L can be attributed to the growth of the amorphous domains and/or sub-domains. This growth may be caused by smaller and/or imperfect PTT crystallites or by coalescence of PTT and/or PEO sub-domains. The tendency of the amorphous sub-domains to grow is supported by a decrease in the miscibility of two amorphous sequences (PTT and PEO) [20].

Based on above results it can be concluded, that the structure of the presented here copolymers is very similar to the supermolecular structure of multiblock copolymers

Table 5
DMTA and tensile properties of PTT-*b*-PEO copolymers.

Sample	E' at 25 °C, MPa	T_β (E''), °C	T_β (tan δ), °C	T_{flow}, °C	E, MPa	σ_y, MPa	ε_y, %	σ_b, MPa	ε_b, %
PTT	2135.5	59α	69α	222	2102.8	–	–	69.3	4.3
PEE-20	433.7	−5	21	210	718.3	31.4	17	29.4	291
PEE-30	178.0	−31	−12	205	371.7	24.0	21	26.7	402
PEE-40	103.1	−41	−28	192	208.5	17.9	24	25.2	468
PEE-50	76.8	−45	−36	177	137.8	13.7	30	21.1	487
PEE-60	56.7	−46	−39	160	87.1	10.3	36	17.4	581
PEE-70	47.6	−48	−43	131	49.0	6.8	46	12.7	680

E', storage modulus at 25 °C; T_β, temperature of β-relaxation corresponding the glass transition determined from maximum of loss modulus (E'') and tan δ; T_{flow}, temperature of softening; E, Young's modulus; σ_y, stress at yield; ε_y, strain at yield; σ_b, stress at break; ε_b, strain at break.

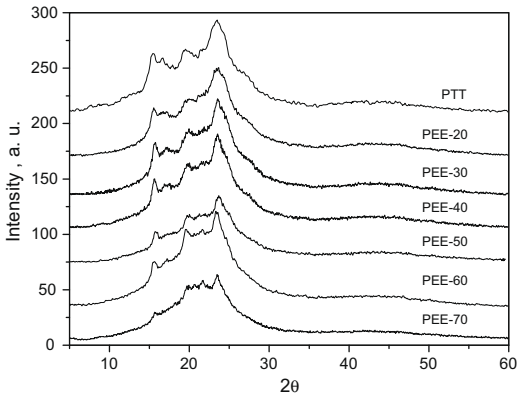

Fig. 9. WAXS patterns for PTT and PTT-*b*-PEO samples.

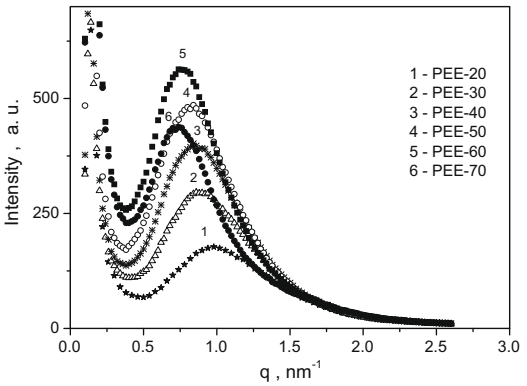

Fig. 10. SAXS curves for PTT-*b*-PEO copolymers.

based on PBT or PET as rigid segments and PTMO as flexible segments. The thermoplastic and elastic behavior of these polymers arise from their multiphase structure, which is a consequence of the chemical nature and incompatibility of the two types of the two contributing segments (rigid and flexible) built into polymer chains. Usually the hydrophilicity and water vapour permeability of segmented block copolymers can be improved by using polar PEO segments instead of hydrophobic flexible segments. The poly(ether-ester)s based on poly(ethylene oxide) (PEO) [34–36] have been shown to have generally worse characteristics than those containing PTMO as the soft segments, but also to have some advantages, the most important being their hydrophilic character, which makes them attractive candidates for some biomedical applications and also in many others application markets like construction, textile, packing. The combination of PEO segments with PTT, which have better tensile elastic recovery than PET and PBT [37,38] can results in elastomers with better energy absorption. Most recently, a large range of polyesters or copolyesters with aliphatic monomeric units of different sizes has been developed. Nevertheless mechanical properties of such polyesters are lower than those of non biodegradable polymers. The PTT-*b*-PEO elastomers seems be good candidate next to PBT-*b*-PEO copolymers already tested [39,40] in tissue engineering which often makes use of biodegradable scaffolds to guide and promote controlled cellular growth and differentiation in order to generate new tissue. Up to now biodegradable polyesters, such polylactide (PLA), poly(glicolide) (PGA), poly(glycolide-co-lactide) (PLGA) were commonly used in tissue engineering. The disadvantage of these biodegradable polyesters is that they undergo plastic deformation and failure when exposed to long-term cyclic strain, limiting their use in engineering elastomeric tissues [41]. For some specific biomedical applications, the PEO was used as flexible segments in multiblock copolyesters based on poly(ε-caprolactone) (PCL) [42], polylactide (PLA)[43], the microbial polyester poly((*R*)-3-hydroxybutyrate) [44], poly(trimetylene carbonate) (PTMC) [45]. Some of them were characterized by improved biodegradability properties, which was depended on the length and content of PEO. These materials have one disadvantage, the oxidative instability during exposure to the light under ambient conditions [46,47]. Besides most of these materials are costly, which is a major hindrance for their wider application. PEO copolymers based on aromatic polyesters is much chipper and biodegradable. Owing to this great advantage, it may have a potential application in mentioned earlier biomedical and also ecological fields. For block copolymers, that contain crystallisable component the interplay between crystallization and microphase separation strongly influences the structural changes, morphology, properties and applications of such materials [20]. To enhance the mechanical properties of copolyesters in terms elasticity, it is preferable to have a strong phase separation between hard and soft phase. In comparison to the poly(ethylene oxide)-*b*-poly(ε-caprolactone) copolymers (PEO-*b*-PCL), where the PEO and PCL have comparable crystallization temperatures and glass transition temperatures, the PTT-*b*-PEO copolymers should have better mechanical properties as a result of better phase separation and also higher thermal and oxidative stability. Unfortunately, they have one disadvantage, being a biomaterial bearing aromatic moieties, the degradation time can be rather much longer than the popular aliphatic polyesters such as poly(glycolide-co-lactide) (PLGA) [42,48], polylactide [43] or poly(butylene terephthalate-co-succinate) [49,50], and only can be tailored in a relatively narrow composition scope [46,51,52].

Table 6
WAXS and SAXS data.

	PTT	PEE-20	PEE-30	PEE-40	PEE-50	PEE-60	PEE-70
x_c, %	34.2	28.3	23.8	20.8	17.0	14.4	6.6
L, nm	7.66	6.28	7.30	7.48	7.66	8.49	8.60

L, long period; x_c, degree of crystallinity determined from WAXS.

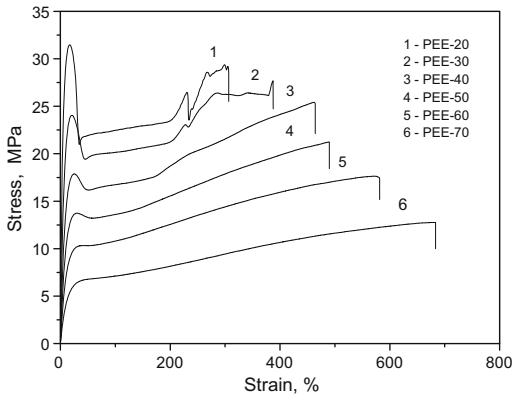

Fig. 11. The stress–strain curves of PTT-*b*-PEO copolymers.

3.3. Tensile properties

Stress–strain curves of the synthesized segmented block copolymers are presented in Fig. 11. Each curve represents the general behavior for several samples tested of a given designation. Values of Young's modulus, yield stress, ultimate strength and elongation of each sample studied are presented in Table 5. By increasing the flexible segment content, the decrease in *E* modulus and in maximum stress with improvement in elongation at break was observed, as a consequence decreasing the number of domains that contribute to the strength. The *E*-modulus was reduced from over 700 MPa for PEE-20 to only 49 MPa for PEE-70 and the maximum stress from 29 to 12 MPa, while the elongation at break for these samples increased from 290% to 680%.

3.4. Thermal stability

The thermal stability of synthesized polymers is an important parameter, which could limit their application. The thermal stability of the synthesized PTT-*b*-PEO copolymers was studied by thermogravimetry under argon and oxidative (air) atmosphere. The TG and derivative TG (DTG) curves in argon and air of the synthesized polymers with different contents of flexible PEO segments are shown in Figs. 12 and 13. The characteristic temperatures for weight losses of 5%, 50%, 25% and 90%, $T_{5\%}$, $T_{25\%}$, $T_{50\%}$, $T_{90\%}$, respectively, in argon and air are given in Table 7. The $T_{5\%}$ value is considered to represent the beginning of thermal degradation. From the shape of the TG and DTG curves, it can be observed that in inert atmosphere (argon) the thermal behaviours of PTT-*b*-PEO copolymers is very similar and practically not dependent on the composition.

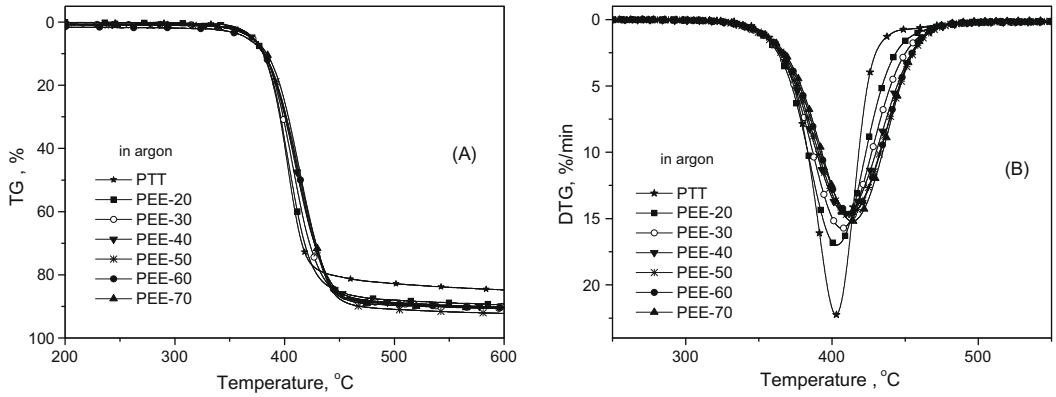

Fig. 12. TG (A) and DTG (B) curves for PTT-*b*-PEO copolymers under argon atmosphere at heating rate 10 °C/min.

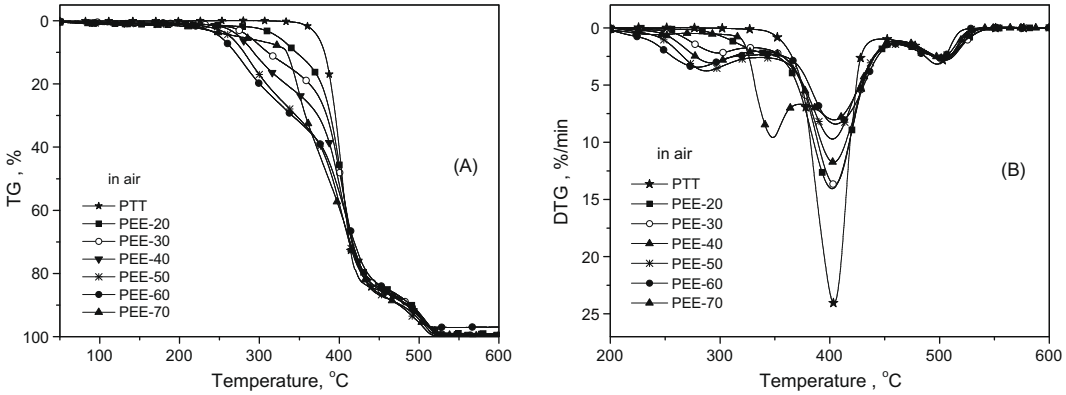

Fig. 13. TG (A) and DTG (B) curves for PTT-*b*-PEO copolymers under air atmosphere at heating rate 10 °C/min.

Table 7
TGA data; temperature of 5%, 25%, 50% and 90% weight loss in argon and air.

Sample	$T_{5\%}$, °C		$T_{25\%}$, °C		$T_{50\%}$, °C		$T_{90\%}$, °C	
	Ar	Air	Ar	Air	Ar	Air	Ar	Air
PTT	371.3	373.3	393.0	392.6	405.0	404.2	–	486.3
PEE-20	371.3	322.9	393.7	384.4	406.5	403.0	579.6	490.6
PEE-30	370.1	287.3	395.5	376.5	410.0	402.1	547.6	488.7
PEE-40	370.7	275.1	396.8	357.2	412.9	398.5	575.7	484.1
PEE-50	369.8	263.7	397.5	326.8	413.6	391.7	469.2	475.1
PEE-60	365.6	250.7	397.9	320.0	414.6	394.8	547.0	489.9
PEE-70	370.7	274.2	400.0	352.1	415.5	386.8	526.6	477.5

Analysis of DTG curves (Fig. 12B) shows that the temperature at the maximum decomposition rate of is shifted to higher temperatures with the increasing the PEO segments content. The PTT homopolymer in air have two stages of degradation, which appear at 350–450 and 450–545 °C. For PTT-*b*-PEO copolymers in air the TG and DTG curves (Fig. 13) reveal different profile, three weight-loss stages occur during degradation. The first and the second stage of the decomposition in air occur in a temperature ranges of 200–350 and 350–460 °C, respectively. The third stage in the temperature range of 460–550 °C is attributed to the decomposition of residue. The first and second stages are attributed to the decomposition of flexible and rigid segments. It is known, that the oxygen attack on poly(ether-ester) block copolymers is initiated in the flexible segment and, in most cases occurs at the α-carbon atom to the ether oxygen atom [53] and results in the formation of volatiles. The values of $T_{5\%}$ and $T_{25\%}$ (first stage) in the series increased with the increase in the content of flexible PEO segments.

4. Conclusions

Series of PTT-*b*-PEO copolymers with different content of flexible PEO segment were synthesized by means of a two-step melt polycondensation process and characterized by various methods. Irganox 1010, a heat stabilizer, was used to protect the polymer chains from thermal degradation during the polycondensation reaction at 255 °C. The rigid segments as well as the flexible ones were randomly distributed along the chain. Due to thermodynamic partial immiscibility of the PTT and the PEO segments, the resulting block copolymers were phase separated, consequently, with domain structure. On the basis of X-ray, DSC and DMTA results, it can be concluded that domains of four types existed in PTT-*b*-PEO copolymers: crystalline PTT, amorphous PTT, amorphous PEO, and amorphous PEO/PTT miscible blend. Crystalline PEO was observed only at temperature below 0 °C for sample containing the highest concentration of PEO segment. The copolymers containing 30–70 wt% of flexible segments have elastomeric property characteristics. The basic structure–property relationship in polyester segmented copolymers states that PTT rigid segments affected the hardness and strength. With respect to the rigid segments content, the melting and crystallization temperature, and the degree of crystallinity decreased with increasing flexible PEO segments content.

Further investigations on elastic properties and morphology depending on the composition and the length of soft segments, with effect of water content and hydrolytic degradation tests are in progress and will be published elsewhere.

Acknowledgements

This work was supported by the Polish Ministry of Science and High Education in the framework of a Grant No. DFG/83/2006 (2007–2009). The author thank Drs. T.A. Ezquerra and A. Nogales from Instituto de Estructura de la Materia C.S.I.C. in Madrid for render access to do WAXS and SAXS measurements, and Shell Chemicals Company for supply 1,3-propanenediol used in synthesis of PTT-*b*-PEO copolymers.

References

[1] Grebowicz JS, Brown H, Chuah H, Olvera JM, Wasiak A, Sajkiewicz P, et al. Polymer 2001;42:7153–60.
[2] Wolfson W. Spinning corncobs into socks farming plastics with "green" chemistry. In: Chemistry & Biology 2006;13:109–11.
[3] Announcement; Bio-sourced packaging materials debut from DuPont (biopolymers). British Plastics & Rubber, Published Online: 1 May 2008.
[4] Eberl A, Heumanna S, Kotekc R, Kaufmannd F, Mitschee S, Cavaco-Paulof A, et al. J Biotechnol 2008;135:45–51.
[5] Kurian J. J Polym Environ 2005;13:159–68; DuPont Tate & Lyle Bio Products begins bio-propanediol production. Focus Surfact 2007; 4–5.
[6] Chuah HH. Synthesis, properties and applications of poly(trimethylene terephthalate). In: Scheirs J, Long TE, editors. Modern polyester: chemistry and technology of polyesters and copolyesters. Chichester, UK: John Wiley Sons; 2004. p. 361–97.
[7] Hong P-D, Chuang W-T, Yeh W-J, Linb T-L. Polymer 2002;43:6879–86.
[8] Chuch HH. Macromolecules 2001;34:6985–93.
[9] Zhang J. J Appl Polym Sci 2004;91:1657–66.
[10] Szymczyk A, Senderek E, Nastalczyk J, Roslaniec Z. Euro Polym J 2008;44:436–43.
[11] Xu Y, Jia H-B, Ye S-R, Huang J. J Mater Sci 2007;42:83811–8385.
[12] Cheng-Fang Ou CH-F. Euro Polym J 2002;38:2405–11.
[13] Dangseeyun N, Supaphol P, Nithitanakul M. Polym Test 2004;23:187–94.
[14] Asadinezhad A, Jafari SH, Khonakdar HA, Böhme F, Hässler R, Häussler L. J Appl Polym Sci 2007;106:1964–71.
[15] Huang JM. J Appl Polym Sci 2003;88:2247–52.
[16] Xu Y, Jia H-B, Piao J-N, Ye S-R, Huang J. J Mater Sci 2008;43:417–21.
[17] Kim KJ, Ramasundaram S, Jong Soon Lee JS. Polym Compos 2008;29:894–901.
[18] Hu X, Lesser AJ. Macromol Chem Phys 2004;205:574–80.
[19] Mishra JK, Chang Y-W, Choi NS. Polym Eng Sci 2007;47:863–70.
[20] Fakirov S. Handbook of condensation thermoplastic elastomers. Weinheim: Wiley-VCH; 2005. p. 77–116, 167–96, 581–97.
[21] Rezwana K, Chena QZ, Blakera JJ, Boccaccini AR. Biomaterials 2006;27:3413–31.

[22] Tirelli N, Lutolf MP, Napoli A, Hubbell JA. Rev Mol Biotechnol 2002;90:3–15.
[23] Deschamps AA, Claasa MB, Sleijster WJ, de Bruijn JD, Grijpma DW, Feijen J. J Control Release 2002;78:175–86.
[24] Van Dijkhuizen-Radersma R, Roosma JR, Sohier J, Flama P, van den Doel M, van Blitterswijk CA, et al. J Bio Mat Res Part A 2004;71A:118–27.
[25] van Dijkhuizen-Radersma R, Roosma JR, Kaim P, Métairie S, Péters FLAMA, de Wijn J, et al. J Biomed Mater Res Part A 2004; 67A:1294–304.
[26] Moroni L, Hendricks JA, Schotel R, de Wijn JR, Van Blitterswijk CA. Tissue Eng 2007;13:361–71.
[27] Chuah HH, Lin-Vien D, Soni U. Polymer 2001;42:7137–9.
[28] Hindeleh AM, Johnson DJ. J Phys (D) 1971;4:259–63;
Hindeleh AM, Johnso DJ. Polymer 1978;19:27–32.
[29] Rabiej M, Rabiej S. Analysis of X-ray diffraction curves of polymers by means of a computer program WAXSFIT (in Polish). Bielsko-Biała (Poland): ATH Press; 2006 [1–132].
[30] Sauer BB, Kampert WG, Blanchard EN, Threefoot SA, Hsiao BS. Polymer 2000;41:1099–108.
[31] Okazaki I, Wunderlich B. Macromol Rapid Commun 1997;18:313.
[32] Brostow W, editor. Performance of Plastics. Munich-Cincinati: Hansher Publishers; 2000 [156–60].
[33] Wang B, Li ChY, Hanzlicek J, Cheng SZD, Geil PH, Grebowicz J, et al. Polymer 2001;42:7171–80.
[34] Deschamps AA, Grijpma DW, Feijen J. Polymer 2001;42:9335–45.
[35] Wang M, Zhang L, Ma D. Eur Polym J 1999;35:1335–43.
[36] Fakirov S, Gogeva T. Macromol Chem 1990;191(615–624):2341–54.
[37] Chen K, Xiaozhen Tang X. J Appl Polym Sci 2003;91:1967–75.
[38] Ward IM, Wilding MA. J Polym Sci Polym Phys 1976;14:263–74.
[39] Radder AM, Leenders H, Van Blitterswijk CA. Biomaterials 1995; 16:507–13.
[40] Waris E, Ashammakhi N, Lehtimäki M, Tulamo RM, Tömälä P, Kellomäki M. Biomaterials 2008;29:2509–15.
[41] Webb A, Yang J, Ameer GA. Informa Pharmaceut Sci 2004;4:801–12.
[42] Hea F, Lia S, Verta M, Zhuo R. Polymer 2003;44:5145–51.
[43] Lee S-H, Soo HK, Han Y-K, KimYoung HA. J Polym Sci Part A Polym Chem 2002;40:2545–55.
[44] Jun L, Xu L, Ni X, Leong KW. Macromolecules 2003;36:2661–7.
[45] Latere Dwan'Isa JP, Rouxhet L, Brewster ME, Préat V, Arie A. Pharmazie 2008;63:235–63.
[46] Deschamps AA DW, Grijpma DW, Feijen J. Polymer 2001; 42:9335–45.
[47] Nagata M, Kiyotsukuri T, Minami S, Tsutsumi N, Sakai W. Polym Intern 1996;39:83–9.
[48] Gan Z, Jim TF, Li M, Yuer Z, Wang S, Wu C. Macromolecules 1999; 32:590–4.
[49] Zhang Y, Feng Z, Feng Q, Cui F. Eur Polym J 2002;40:1297–308.
[50] Pepić D, Radoičić M, Adoičić MS, Nikolić MS, Djonlaiić J. J Serb Chem Soc 2007;72:1515–31.
[51] Kumar N, Ravikumar MNV, Domb AJ. Adv Drug Delivery Rev 2001;53:23–44.
[52] Södergard A, Stolt M. Prog Polym Scie 2002;27:1123–63.
[53] Szymczyk A, Rosłaniec Z. Polimery (Warsaw) 2006;51:627–42.